Antipolar phase in multiferroic $BiFeO_3$ at high pressure

D. P. Kozlenko,[1,*] A. A. Belik,[2] A. V. Belushkin,[1] E. V. Lukin,[1] W. G. Marshall,[3]
B. N. Savenko,[1] and E. Takayama-Muromachi[2]

[1]*Frank Laboratory of Neutron Physics, JINR, 141980 Dubna, Russia*

[2]*International Center for Materials Nanoarchitectonics (MANA), National Institute for Materials Science (NIMS), 1-1 Namiki, Tsukuba, Ibaraki 305-0044, Japan*

[3]*ISIS Facility, STFC Rutherford Appleton Laboratory, Harwell Science and Innovation Campus, Harwell Oxford, Oxon, OX11 0QX, United Kingdom*

(Received 22 June 2011; published 19 September 2011)

The crystal and magnetic structures of $BiFeO_3$ have been studied at high pressures up to 8.6 GPa by means of neutron powder diffraction at ambient temperature. Upon compression, a reduction of the spontaneous ferroelectric polarization is evidenced from the analysis of atomic displacements in the rhombohedral phase. A structural phase transition from the polar rhombohedral $R3c$ phase to the antipolar orthorhombic $Pbam$ phase with antiferroelectic character of atomic displacements was revealed at $P = 3$ GPa. The lattice parameters of the $Pbam$ phase at $P = 4.1$ GPa are $a = 5.5177(4)$, $b = 11.159(1)$ and $c = 7.7550(6)$ Å. The variation of the structural parameters of both phases as a function of pressure was determined. The initially incommensurate G-type antiferromagnetic structure of $BiFeO_3$ becomes commensurate due to the structural phase transition.

DOI: 10.1103/PhysRevB.84.094108 PACS number(s): 77.80.B−, 61.50.Ks, 75.25.−j, 75.85.+t

I. INTRODUCTION

The multiferroic materials, exhibiting coexistence of polar and magnetic orders, are the focus of extensive current scientific research.[1,2] Particular attention has been given to understanding the origin of magnetoelectric coupling, which provides a way to control magnetic properties of materials by application of an electric field and vice versa, and is important technologically for the development of novel applications.[3–5]

$BiFeO_3$ is one of the most promising multiferroic materials for both fundamental and applied research, as this material exhibits both polar and magnetic order well above ambient temperature.[1,6] In this compound, the ferroelectricity is induced by a stereochemically active $6s^2$ lone pair of the Bi^{3+} ions. The polar rhombohedral $R3c$ phase is formed in $BiFeO_3$ below the Curie temperature $T_C = 1100$ K.[7] The ferroelectric polarization reaches a value of about 100 $\mu C/cm^2$ for single crystals at ambient temperature.[8] The incommensurate G-type antiferromagnetic (AFM) order with cycloidal modulation occurs in $BiFeO_3$ below the Néel temperature $T_N = 640$ K.[9,10] The presence of strong magnetoelectric coupling in $BiFeO_3$ was proved by observation of electrical control of the AFM domain structure.[11]

Recently the existence of novel high-pressure phases of $BiFeO_3$ was deduced from synchrotron radiation diffraction and far-infrared spectroscopy studies.[12,13] In the structural study,[12] the transformations to a monoclinic phase of $C2/m$ symmetry at $P \sim 3$ GPa and orthorhombic phase of the $Pnma$ symmetry at $P \sim 10$ GPa were found. In contrast, two high-pressure orthorhombic phases were found to appear in $BiFeO_3$ at $P \sim 4$ and 8 GPa in the structural study.[13] The reflection conditions of these phases afford maximal space groups $Immm$ and $Ibam$, respectively.

Although the proposed structural models[12,13] of the intermediate high-pressure phase of $BiFeO_3$ are distinct, they predict a nonpolar character to this phase and modification of the magnetoelectric coupling upon compression. In order to clarify the nature of the crystal structure of the high-pressure phase of $BiFeO_3$ and study the effect of high pressure on the magnetic order of $BiFeO_3$, we have performed a neutron powder diffraction study over the 0–8.6 GPa pressure range.

II. EXPERIMENTAL

The $BiFeO_3$ was synthesized from a stoichiometric mixture of Bi_2O_3 (99.9999%) and Fe_2O_3 (99.9999%). Mixed powders were pressed into pellets and annealed at 1073 K in air for 2 h on Pt plates with subsequent quenching into air. One pellet was used to prevent the direct contact between the Pt plate and the remaining part of the sample because of a possible reaction between Pt and Bi_2O_3. The heating time to 1073 K was 2 h.

The crystal and magnetic structures of $BiFeO_3$ in the pressure range 0–8.6 GPa at ambient temperature were studied using the HiPr diffractometer (ISIS, RAL, UK) and the Paris-Edinburgh pressure cell.[14] The sample was loaded in the TiZr encapsulated gasket of 75 mm^3 initial volume.[15] A small amount of polycrystalline CaF_2 was added to the sample to act as a suitable pressure marker.[16] The 4:1 volume mixture of fully deuterated methanol-ethanol was used as a pressure transmitting medium to attain nearly hydrostatic compression of the sample over the studied pressure range. Time-of-flight neutron powder diffraction patterns were collected in the transverse scattering geometry using the main HiPr detector bank covering the scattering angle range $83^\circ < 2\theta < 97^\circ$. Additional measurements at selected pressures were performed in the longitudinal scattering geometry using the single detector module covering the scattering angle range $20^\circ < 2\theta < 40^\circ$. A typical data collection time was about 3 h.

The diffraction data for both the crystal and magnetic structure were analyzed by the Rietveld method using the FULLPROF program.[17]

III. RESULTS AND DISCUSSION

The neutron diffraction patterns of $BiFeO_3$ measured at selected pressures and ambient temperature are shown in

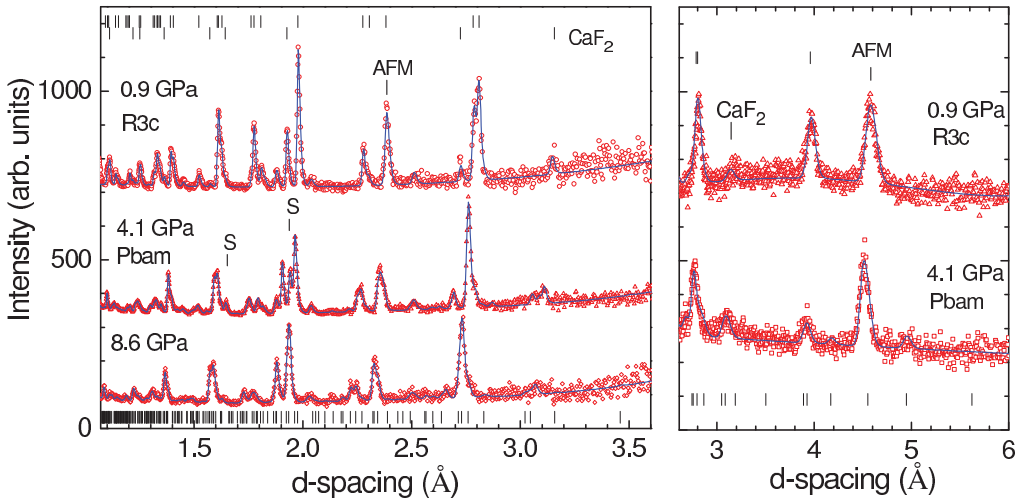

FIG. 1. (Color online) Neutron diffraction patterns of $BiFeO_3$ measured at selected pressures and ambient temperature using the HiPr detector banks located at scattering angles $2\theta = 90°$ (left) and 30° (right), and processed by the Rietveld method. Experimental points and calculated profiles are shown. Tickmarks at the top represent the calculated positions of nuclear structure peaks of the ambient pressure rhombohedral phase (upper row) and the CaF_2 pressure marker (lower row). The tickmarks at the bottom represent the calculated positions of the nuclear peaks of the high-pressure *Pbam* orthorhombic phase. The characteristic superstructure peaks of the orthorhombic phase are marked with an S. The most intense peaks with dominant magnetic contribution are marked as AFM.

Fig. 1. For the pressure range 0–3 GPa, the observed patterns were consistent with the known *R*3*c* rhombohedral phase of $BiFeO_3$. The structural parameters obtained at ambient pressure (Table I) are close to those reported previously.[18,19] The compression of the unit cell is anisotropic with the most compressible direction being the *c* axis (Fig. 2). The lattice parameters ratio $c/a\sqrt{6}$, which reflects the distortion of the pseudocubic perovskite subcell, varies from 1.015 ($P = 0$ GPa) to 1.008 ($P = 2.6$ GPa). The volume compressibility data (Fig. 2) were fitted by the third-order Birch–Murnaghan equation of state:[20]

$$P = \tfrac{3}{2}B_0(x^{-7/3} - x^{-5/3})\left[1 + \tfrac{3}{4}(B' - 4)(x^{-2/3} - 1)\right],$$

where $x = V/V_0$ is the relative volume change, V_0 is the unit cell volume at $P = 0$, and B_0, B' are the bulk modulus $[B_0 = -V(dP/dV)_T]$ and its pressure derivative $[B' = (dB_0/dP)_T]$. The fitted values $B_0 = 100(5)$ GPa, $B' = 4.0(5)$ and unit cell volume per formula unit $V_0 = 62.35(5)$ Å^3 are consistent with previous studies.[12,13] The average Fe-O bond length decreases nearly linearly upon compression (Fig. 3), the calculated linear compressibility coefficient $k_{Fe-O} = -[1/(l_{Fe-O})_{P=0}](dl_{Fe-O}/dP)_T$ is $k_{Fe-O} = 0.0028$ GPa^{-1}.

The value of the spontaneous ferroelectric polarization produced by ionic displacements can be calculated as $P_s = \Sigma(m_i \Delta x_i Z_i)e/V$, where m_i is the crystallographic site multiplicity, Δx_i is the ionic displacement along the polar axis from the position in the paraelectric phase, $Z_i e$ is the formal charge of the *i*th ion, and summation is taken over all ions located in the unit cell volume *V*.[21] The calculated value of $P_s = 94$ μC/cm^2 at ambient pressure is consistent with experimental observations.[8] Upon compression, a gradual reduction of the P_s value occurs (Fig. 4), implying an instability of the polar phase.

The G-type AFM order of $BiFeO_3$ is indicated by the presence of a purely magnetic peak located at 4.58 Å and a noticeable magnetic contribution to a reflection located at 2.39 Å in the diffraction patterns (Fig. 1). The incommensurate model of the G-type AFM order,[10,22] with the propagation vector $k = (\delta, \delta, 0)$ results in somewhat better *R* factors of fitting quality of the diffraction data with respect to the simplified commensurate model, although the medium resolution of the diffraction data did not allow us to resolve the magnetic satellite peaks. The values of the propagation vector components $\delta = 0.004(1)$ and the ordered magnetic moment of Fe ions $\mu_{Fe} = 4.0(1)$ μ_B, obtained at ambient conditions, are consistent with those determined in high resolution neutron diffraction experiments.[10,22] The δ value remains about the same in the 0–3 GPa pressure range.

At pressures above 3 GPa, noticeable changes in the diffraction data were observed (Fig. 1), indicating the onset of a structural phase transition. We applied the previously proposed *C*2/*m* (Ref. 12) and *Cmmm* (Ref. 13) structural models for the high-pressure phase. The orthorhombic *Cmmm* model with the $\sqrt{2}a_p \times 3\sqrt{2}a_p \times a_p$ superstructure (a_p is the parameter of the simple perovskite subcell) provided a rather poor fit to the diffraction data by the Rietveld method, yielding *R*-factor values $R_p = 9.24$, $R_{wp} = 10.9\%$ (for the pattern measured at $P = 4.1$ GPa). The monoclinic *C*2/*m* model with the $2\sqrt{5}\,a_p \times 2a_p \times \sqrt{2}\,a_p$ superstructure resulted in a better quality of fit with the $R_p = 7.59$, $R_{wp} = 5.95\%$, but the intensities of several diffraction peaks were described unsatisfactorily. Detailed analysis of the diffraction data shows that the full set of the observed reflections of the high-pressure phase can be alternatively indexed using the orthorhombic $\sqrt{2}a_p \times 2\sqrt{2}a_p \times 2a_p$ superstructure of *Pbam* symmetry. Application of the *Pbam* structural model (Fig. 5) provides the best fitting of the diffraction data (Fig. 1), with final *R*-factor values of $R_p = 6.21$, $R_{wp} = 4.95\%$. In

TABLE I. Structural parameters of the rhombohedral and orthorhombic phases of $BiFeO_3$ at selected pressures and ambient temperature. The R_p and R_{wp} factor values are also given.

P, GPa	0	2.1	4.1	6.4
Symmetry	*R*3*c*	*R*3*c*	*Pbam*	*Pbam*
Lattice parameters				
a, Å	5.5797(3)	5.5547(3)	5.5177(4)	5.4638(8)
b, Å			11.159(1)	11.087(2)
c, Å	13.874(1)	13.723(1)	7.7550(6)	7.7158(9)
Atomic coordinates				
Bi1: *x*	0	0	0.705(3)	0.731(4)
y	0	0	0.128(1)	0.116(2)
z	0	0	0	0
Bi2: *x*			0.708(3)	0.714(4)
y			0.129(1)	0.123(2)
z			0.5	0.5
Fe: *x*	0	0	0.256(1)	0.264(2)
y	0	0	0.119(1)	0.124(2)
z	0.2210(4)	0.2229(5)	0.246(1)	0.248(2)
O1: *x*	0.449(1)	0.446(1)	0.302(4)	0.279(5)
y	0.023(1)	0.022(1)	0.156(2)	0.158(3)
z	0.9522(6)	0.9553(7)	0	0
O2: *x*			0.314(4)	0.315(5)
y			0.075(2)	0.071(3)
z			0.5	0.5
O3: *x*			0.058(2)	0.064(3)
y			0.266(1)	0.270(2)
z			0.272(2)	0.277(3)
O4: *x*			0	0
y			0.5	0.5
z			0.329(2)	0.314(3)
O5: *x*			0	0
y			0	0
z			0.234(2)	0.223(3)
R-factors				
R_p,%	9.02	9.69	6.21	9.71
R_{wp},%	6.61	6.99	4.95	7.59

order to check possible phase coexistence, additional trial refinements for a combination of the *Pbam* model with the *C*2/*m* and *Cmmm* models were made. It was found that the single phase *Pbam* model provides the best description of the experimental high-pressure data. The structural parameters of the rhombohedral and orthorhombic phases of $BiFeO_3$ obtained from Rietveld refinement of the diffraction data at selected pressures are listed in Table I.

The *Pbam* symmetry of the high-pressure phase crystal structure allows antipolar ionic displacements, and it is observed in the antiferroelectric $PbZrO_3$ at ambient pressure.[23] The structurally similar antipolar phases were also found in substituted $Bi_{1-x}R_xMnO_3$ compounds (R = La, Nd, Sm) for $x \sim 0.14$–0.20 at ambient pressure.[24–28] The origin of the *R*3*c*-*Pbam* transition should be related to the complex interplay of structural distortions due to the stereochemically active $6s^2$ lone pair of the Bi^{3+} ions and rotations of FeO_6 octahedra,[29,30] as modified by compression. The octahedral tilt system at the phase transition changes from $a^-a^-a^-$ to $a^-a^-c^0$ in the Glazer notation.[31] Recent first-principles theoretical studies have predicted a number of tetragonal,

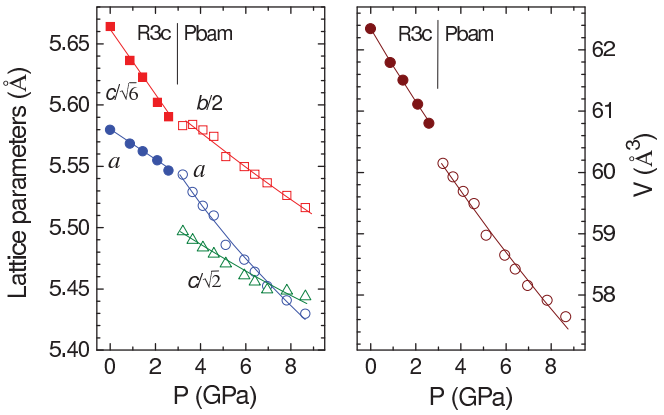

FIG. 2. (Color online) Lattice parameters (left) and unit cell volume per formula unit (right) as functions of pressure in the rhombohedral and orthorhombic phases of $BiFeO_3$.

monoclinic, and orthorhombic potentially stable low-energy polar phases of $BiFeO_3$,[32–34] and some of them were found to exist under epitaxial strain in thin films.[35] However, the stability conditions for the antipolar phase in $BiFeO_3$ remain less explored and require further theoretical considerations.

The lattice compression of the *Pbam* phase is anisotropic with the most compressible *a* unit cell parameter (Fig. 2). The values of the bulk modulus $B_0 = 99(5)$ GPa and its pressure derivative $B' = 4.0(5)$ obtained from the fitting of volume compressibility data are about the same as for the ambient pressure polar phase, while the unit cell volume per formula unit extrapolated to zero pressure, $V_0 = 61.97$ Å^3, is slightly reduced by 0.6%. The compression of the average Fe-O bond length value (Fig. 3) is approximately linear but with a larger compressibility $k_{Fe-O-HP} = 0.0042$ GPa^{-1} in comparison with the rhombohedral phase.

Analysis of the atomic coordinates (Table I) of the orthorhombic phase of $BiFeO_3$ at $P = 4.1$ GPa shows that the Bi ions exhibit significant shifts from the centrosymmetric positions by about 0.24 Å along the *a* axis and 0.03 Å along the *b* axis. The centers of gravity of the oxygen coordination shells around the Bi ions, composed of 12 O atoms, are shifted

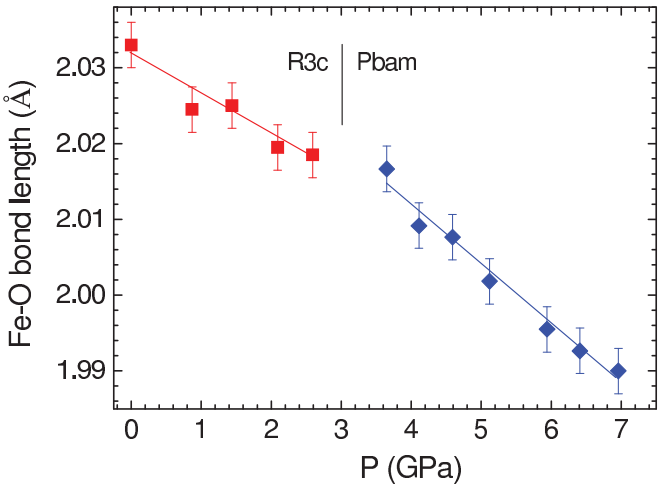

FIG. 3. (Color online) The average Fe-O bond length as a function of pressure in the rhombohedral and orthorhombic phases of $BiFeO_3$.

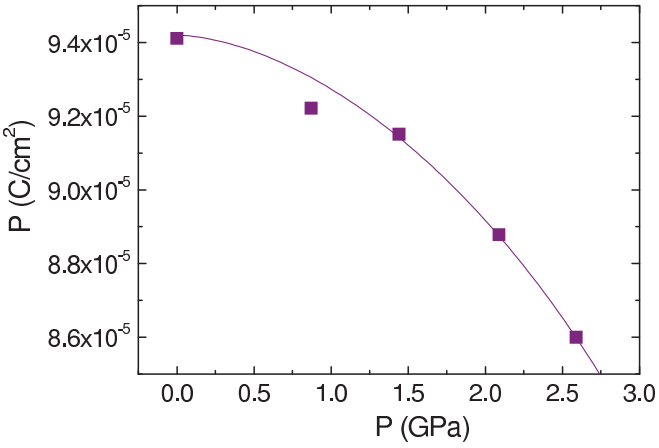

FIG. 4. (Color online) The calculated spontaneous ferroelectric polarization produced by ionic displacements in the rhombohedral phase of $BiFeO_3$ as a function of pressure. The line is a guide to the eye only.

from the centrosymmetric positions in the opposite direction by about 0.15 Å along the *a* axis. The centers of gravity of the iron coordination shells around the Bi ions, composed of eight Fe atoms, nearly coincide with the centrosymmetric positions. This provides evidence of the electric dipole formation in the orthorhombic high-pressure phase of $BiFeO_3$ and their antipolar arrangement (Fig. 5), leading to an antiferroelectric nature for this phase.

The magnetic contribution to the neutron diffraction data of the high-pressure phase of $BiFeO_3$ was qualitatively similar to that for the initial rhombohedral phase (Fig. 1), and refinements of the magnetic structure began once again with the G-type incommensurate AFM order with propagation vector $k = (\delta,\delta,0)$.[10,22] The value $\delta = 0.000(2)$ was obtained for the pressure range 4.1–8.6 GPa, implying a commensurate character for the G-type AFM order in the orthorhombic *Pbam* phase of $BiFeO_3$. The refined value of the ordered magnetic moments of Fe ions, $\mu_{Fe} = 5.0(1)\ \mu_B$ at $P = 4.1$ GPa and ambient temperature, is somewhat larger in comparison with that obtained for the rhombohedral phase.

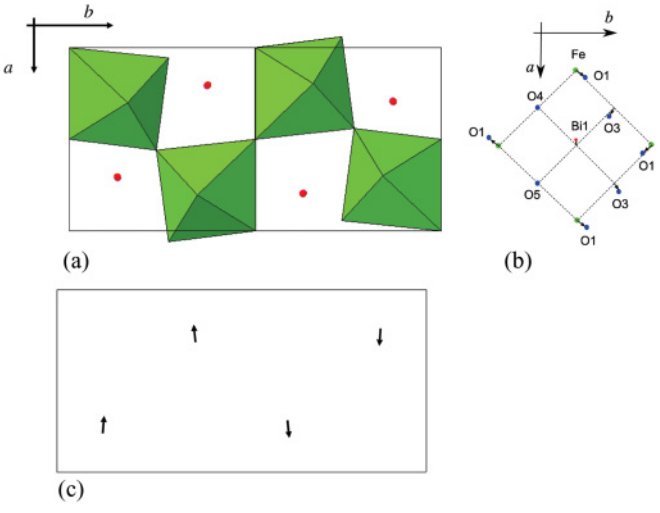

FIG. 5. (Color online) The *Pbam* orthorhombic crystal structure of the high-pressure phase of $BiFeO_3$, viewed along the crystallographic *c* axis. (a) The FeO_6 octahedra and Bi ions located between them are shown. (b) The ionic displacements from centrosymmetric positions, illustrated in the vicinity of the Bi1 ion with coordinates listed in Table I, giving rise to the formation of the electric dipole moments. (c) A schematic representation of the antipolar arrangement of the electric dipole moments in the *Pbam* structure.

A detailed theoretical analysis of the magnetoelectric properties of $BiFeO_3$ has shown[36] that the absolute values of the propagation vector *k* of the AFM state and spontaneous ferroelectric polarization P_z are related as

$$k = \gamma P_s / 2J,$$

where γ is the magnetoelectric coefficient, and J is the magnetic superexchange interaction strength. This relation implies, therefore, that the commensurate character of the AFM order is a direct consequence of the antipolar nature of the high-pressure phase of $BiFeO_3$ with $P_s = 0$.

In the x-ray diffraction study,[13] another structural phase transition in $BiFeO_3$ was detected on compression above 7.5 GPa. The $\sqrt{2}a_p \times 3\sqrt{2}a_p \times 2a_p$ superstructure was assumed for this phase. However, due to technical restrictions the accessible pressure range in our neutron diffraction experiments was limited to 8.6 GPa, comparable with the transition pressure, and we were not able to observe any signature of this phase transition. Recently, it was shown that the nonhydrostatic stress is an important parameter, modifying the sequence of the phase transitions and transition pressures in $BiFeO_3$.[37] Therefore, a possible reason for the difference in the present results and synchrotron radiation diffraction data[12,13] is the distinctive nonhydrostatic stress conditions due to application of different pressure transmitting media.

IV. CONCLUSIONS

The results of our study demonstrate that application of high pressure leads to a suppression of the spontaneous ferroelectric polarization in the polar rhombohedral phase of *R*3*c* symmetry, followed by a structural phase transition to an antipolar orthorhombic phase of *Pbam* symmetry at $P \sim 3$ GPa. This transition occurs due to a complex interplay of pressure-induced structural distortions, related to the stereochemically active $6s^2$ lone pair of the Bi^{3+} ions and rotations of FeO_6 octahedra.

As a result of the polar-antipolar phase transition, the G-type AFM order becomes commensurate, in accordance with theoretical models of magnetoelectric coupling of $BiFeO_3$.

ACKNOWLEDGMENTS

This paper has been partially supported by the Russian Foundation for Basic Research, Grant 09-02-00311-a, the Ministry of Education and Science of Russian Federation, state contracts No. 02.740.11.0542 and No. 16.518.11.7029, World Premier International Research Center Initiative (MEXT, Japan), the Japan Society for the Promotion of Science through its Funding Program for World-Leading Innovative R&D on Science and Technology (FIRST Program), and the Grants-in-Aid for Scientific Research (22246083). The allocation of beamtime and financial support of the ISIS and STFC (UK) is gratefully acknowledged. The authors also thank C. Barry for technical assistance.

*Corresponding author: denk@nf.jinr.ru

[1] G. A. Smolenskii and I. E. Chupis, Sov. Phys. Usp. **25**, 475 (1982).
[2] T. Kimura, T. Goto, H. Shintani, K. Ishizaka, T. Arima, and Y. Tokura, Nature **426**, 55 (2003).
[3] M. Fiebig, J. Phys. D **38**, R123 (2005).
[4] N. A. Spaldin and M. Fiebig, Science **309**, 391 (2005).
[5] W. Eerenstein, N. D. Mathur, and J. F. Scott, Nature **442**, 759 (2006).
[6] G. Catalan and J. F. Scott, Adv. Mater. **21**, 2463 (2009).
[7] G. A. Smolenskii, V. A. Isupov, A. I. Agranovskaya, and N. N. Krainik, Sov. Phys. Solid State **2**, 2651 (1961).
[8] D. Lebeugle, D. Colson, A. Forget, and M. Viret, Appl. Phys. Lett. **91**, 022907 (2007).
[9] G. A. Smolenskii, V. Yudin, E. Sher, and Yu. E. Stolypin, Sov. Phys. JETP **16**, 622 (1963).
[10] I. Sosnowska, T. Peterlin-Neumaier, and E. Steichele, J. Phys. C: Solid State Phys. **15**, 4835 (1982).
[11] T. Zhao, A. Scholl, F. Zavaliche, K. Lee, M. Barry, A. Doran, M. P. Cruz, Y. H. Chu, C. Ederer, N. A. Spaldin, R. R. Das, D. M. Kim, S. H. Baek, C. B. Eom, and R. Ramesh, Nature Mater. **5**, 823 (2006).
[12] R. Haumont, P. Bouvier, A. Pashkin, K. Rabia, S. Frank, B. Dkhil, W. A. Crichton, C. A. Kuntscher, and J. Kreisel, Phys. Rev. B **79**, 184110 (2009).
[13] A. A. Belik, H. Yusa, N. Hirao, Y. Ohishi, and E. Takayama-Muromachi, Chem. Mater. **21**, 3400 (2009).
[14] J. M. Besson, R. J. Nelmes, G. Hamel, J. S. Loveday, G. Weill, and S. Hull, Physica B **180/181**, 907 (1992).
[15] W. G. Marshall and D. J. Francis, J. Appl. Crystallogr. **135**, 122 (2002).
[16] R. J. Angel, J. Phys. Condens. Matter **5**, L141 (1993).
[17] J. Rodríguez-Carvajal, Physica B **192**, 55 (1993).
[18] P. Fischer, M. Polomska, I. Sosnowska, and M. Szymanski, J. Phys. C: Solid State Phys. **13**, 1931 (1980).
[19] A. Palewicz, R. Przenioslo, I. Sosnowska, and A. W. Hewat, Acta Cryst. B **63**, 537 (2007).
[20] F. J. Birch, J. Geophys. Res. **91**, 4949 (1986).
[21] M. Avdeev, J. D. Jorgensen, S. Short, G. A. Samara, E. L. Venturini, P. Yang, and B. Morosin, Phys. Rev. B **73**, 064105 (2006).
[22] R. Przenioslo, M. Regulski, and I. Sosnowska, J. Phys. Soc. Jpn. **75**, 084718 (2006).
[23] A. M. Glazer, K. Roleder, and J. Dec, Acta Cryst. B **49**, 846 (1993).
[24] S. Karimi, I. M. Reaney, Y. Han, J. Pokorny, and I. Sterianou, J. Mater. Sci. **44**, 5102 (2009).
[25] I. Levin, S. Karimi, V. Provenzano, C. L. Dennis, H. Wu, T. P. Comyn, T. J. Stevenson, R. I. Smith, and I. M. Reaney, Phys. Rev. B **81**, 020103 (2010).
[26] I. O. Troyanchuk, D. V. Karpinsky, M. V. Bushinsky, V. A. Khomchenko, G. N. Kakazei, J. P. Araujo, M. Tovar, V. Sikolenko, V. Efimov, and A. L. Kholkin, Phys. Rev. B **83**, 054109 (2011).
[27] D. A. Rusakov, A. M. Abakumov, K. Yamaura, A. A. Belik, G. Van Tendeloo, and E. Takayama-Muromachi, Chem. Mater. **23**, 285 (2011).
[28] I. Levin, M. G. Tucker, H. Wu, V. Provenzano, C. L. Dennis, S. Karimi, T. Comyn, T. Stevenson, R. I. Smith, and I. M. Reaney, Chem. Mater. **23**, 2166 (2011).
[29] D. J. Singh, M. Ghita, M. Fornari, and S. V. Halilov, Ferroelectrics **338**, 73 (2006).
[30] O. Dieguez, O. E. Gonzalez-Vazquez, J. C. Wojdel, and J. Iniguez, Phys. Rev. B **83**, 094105 (2011).
[31] A. M. Glazer, Acta Cryst. B **28**, 3384 (1972).
[32] C. Ederer and N. A. Spaldin, Phys. Rev. Lett. **95**, 257601 (2005).
[33] B. Dupé, I. C. Infante, G. Geneste, P. E. Janolin, M. Bibes, A. Barthélémy, S. Lisenkov, L. Bellaiche, S. Ravy, and B. Dkhil, Phys. Rev. B **81**, 144128 (2010).
[34] O. Diéguez, O. E. González-Vázquez, J. C. Wojdeł, and J. Íñiguez, Phys. Rev. B **83**, 094105 (2011).
[35] I. C. Infante, S. Lisenkov, B. Dupé, M. Bibes, S. Fusil, E. Jacquet, G. Geneste, S. Petit, A. Courtial, J. Juraszek, L. Bellaiche, A. Barthélémy, and B. Dkhil, Phys. Rev. Lett. **105**, 057601 (2010).
[36] A. M. Kadomtseva, A. K. Zvezdin, Yu. F. Popov, A. P. Pyatakov, and G. P. Vorob'ev, JETP Lett. **79**, 571 (2004).
[37] M. Guennou, P. Bouvier, R. Haumont, G. Garbarino, and J. Kreisel, Phase Transitions **84**, 474 (2011).